



# Mathematical Models of Chiral Symmetry-breaking – A Review of General Theories, and Adiabatic Approximations of the APED System

Priscila C. Diniz<sup>1</sup> · Jonathan A. D. Wattis<sup>2</sup> · Fernando P. da Costa<sup>1</sup>

Received: 7 September 2022 / Accepted: 17 October 2022 / Published online: 23 November 2022  
© The Author(s) 2022

## Abstract

We review the literature surrounding chiral symmetry-breaking in chemical systems, with a focus on understanding the mathematical models underlying these chemical processes. We comment in particular on the toy model of Sandars, Viedma's crystal grinding systems and the APED model. We include a few new results based on asymptotic analysis of the APED system.

**Keywords** Origins of Life · Homochirality · APED · Mathematical Models · Bifurcation theory

## Introduction

Chiral symmetry-breaking concerns the formation of complicated molecules that can exist in left-handed or right-handed form, such as DNA, polymers, sugars, and many chemicals necessary for life to exist. Typically, only one form of these chemicals is observed in nature, for example, DNA and sugars are right-handed, whilst amino acids, the main components of proteins in the human body, are all left-handed. We use the terminology *R* for right-handed, and *L* for left; although *D* and *L* are also found in the literature; *R* being replaced by *D* for the latin term *dexter*, and *L* for *levo*. The term “chiral” comes from the Greek *cheiral*, which means “hand”. Originally, the

---

Jonathan A. D. Wattis and Priscila C. Diniz contributed equally to this work.

---

✉ Jonathan A. D. Wattis  
Jonathan.Wattis@nottingham.ac.uk

Priscila C. Diniz  
epriscila.diniz@gmail.com

Fernando P. da Costa  
Fernando.Pestana.Costa@tecnico.ulisboa.pt

<sup>1</sup> Department of Science and Technology, Universidade Aberta, Palácio Ceia, Rua da Escola Politécnica 141-147, 1269-001 LISBOA, State, Portugal

<sup>2</sup> Centre for Mathematical Medicine and Biology, School of Mathematical Sciences, University of Nottingham, University Park, Nottingham NG7 2RD, UK

classification was based on chiral molecules rotating the plane of polarized light. If the plane of polarized light is rotated clockwise as it approaches the observer (to the right), the molecule is dextrorotatory (*D*). If the plane of polarized light is rotated counterclockwise (to the left), the molecule is levorotatory (*L*).

In chemistry, the term “enantiomers” is used to describe molecules that have the following key characteristics: the molecule is asymmetric (that is, it has no axis of symmetry), enantiomers are then mirror images of one another, and enantiomers are not superimposable, either by rotation nor by translation. A racemic mixture (or racemate) is a mixture of equal amounts of two enantiomers of a chiral molecule, whose optical activity shifts the plane of polarized light nor neither to the left, nor the right. In a mixture, the degree of chirality can be described by a quantity known as the enantiomeric excess, which is defined by the ratio of the difference in concentrations to their sum, specifically

$$ee = \frac{[R] - [L]}{[R] + [L]}, \quad (1)$$

which has the property  $-1 \leq ee \leq +1$ . An enantiomerically pure substance has  $\pm 100\%$  enantiomeric excess (*ee*), and can be described as homochiral, whilst racemic mixtures have  $ee = 0$ .

In this paper, we are concerned with the formation of larger clusters which have a chiral structure, whether these structures be crystals or polymers or some other form of agglomeration. The structure may arise due to (i) the aggregation of chiral monomers; we will only be interested in these systems if there is process whereby left-handed monomers can transform into right-handed monomers and vice versa (i.e.  $L_1 \rightleftharpoons R_1$ ), so that chiral end state could arise from a racemic initial conditions; alternatively, (ii) clusters may have a chiral structure purely due to the arrangement of achiral monomers. Chiral structures arise in both organic and inorganic compounds.

The area of chiral systems is vast - encompassing both experimental and theoretical work, covering biological, chemical and physical systems. Ribo et al. (2017) review chemical systems which can spontaneously break the left-right mirror symmetry, whether this is in ‘open’ systems such as that proposed by Frank (1953), or ‘closed’ processes, such as Viedma’s crystal grinding experiments, or more complicated hypercycles (Ribo et al. 2017). A broad-ranging review of the models of homochirality in far-from-equilibrium systems is given by Plasson et al. (2007), who cover general models, both those fixed mass which is recycled and those with input and outflow of mass. They discuss autocatalysis, competition, inhibition, positive and negative feedback, and consider APED as one example. Other relevant reviews include Coveney et al. (2012) and Wattis and Coveney (2005b).

Since it has been relatively well-served by review articles, here, we only give a brief overview of the wider area “Origins”, covering the origins of life motivation, early experimental and theoretical models. “Chiral Crystallisation Experiments” provides a discussion of Chiral crystallisation experiments and associated mathematical models, before focusing on the APED system in “The APED Model”. We present some new results on the bifurcations in the APED model, with more extensive analysis of a generalised APED model to be presented in later work (Diniz et al. 2023).

## Origins

### Origins of Life

In 1953, Miller (1953) and Urey (1952) aimed to recreate the supposed conditions of the early Earth, following Oparin (1938) and Haldane (1929). Starting from simple molecules of ammonia, hydrogen, methane and water vapor, they imposed extreme conditions of heat and electrical discharges, and produced a mix of amino acids, urea, hydroxy and short aliphatic acids. Repeated experiments resulted in relatively high yields of a few biologically relevant molecules. Lazcano and Bada (2003) provide a history of the experiments and a reflection on their subsequent impact. This is relevant to the topic of this paper, since amino acids aggregate into chiral structures, as investigated by Hitz et al. (2001). One may expect systems to be dominated by copolymers containing approximately equal numbers of L and R, however, one may find unexpectedly large numbers of homopolymers. The results obtained from such systems have been analysed by Wattis and Coveney (2007) and Blanco and Hochberg (2012), who show that relatively simple differences between homopolymerisation (R-R, L-L) and heteropolymerisation (L-R, R-L) can help explain the formation of high levels of homopolymers. For more details on the important role of block copolymers in cell-like structures relevant to the origins of life, the reader is directed to the review by Fuks et al. (2011).

Gleiser et al. (2012) consider systems of chiral polymerisation reactions with chirally-selective reaction rates, but no explicit autocatalysis or enantiomeric cross-inhibition. Their model allows general heteropolymers to form, that is, polymers consisting of  $i$  left-monomers and  $j$  right-monomers, where  $(i, j)$  can be any numbers. The rate of addition of  $L$ -monomers may differ from that of  $R$ -monomers. Similarly, the rate of depolymerisation rates may differ, that is, the dissociation rates of  $L$  and  $R$  monomers can differ. Their aim is to determine how much explicit selectivity is required for the whole system to become homochiral. They find that even with a chiral bias of less than 10%, the system can evolve to a high global enantiomeric excess ( $ee$ ), that is, a state in which the concentrations of one handedness significantly exceeds the other.

Walker (2017) has explored the origins of life issue in more detail, highlighting the many and diverse key ideas that have yet to be integrated into a single physical theory. Models for the separate processes have been considered various authors, for example, Eigen (1971), Eigen and Schuster (1982), Coveney et al. (2012), and Wattis and Coveney (2005b). Chen and Ma (2020) have recently discussed, and provided simulations of models which explore the inter-relation of homochirality with the RNA world hypothesis. Their interpretation of the results is that homochirality and the RNA world arose simultaneously, and it is not necessary to assume that homochirality of monomers occurred before the formation of RNA.

Hochberg et al. (2017) applies stoichiometric network analysis (SNA) – a theoretical approach for general networks to systems with mirror symmetry to investigate conditions for symmetry-breaking. Results in the analysis of multiple large matrices, for example,  $11 \times 7$  for the simplest Frank model, and  $18 \times 12$  for a simple limited enantioselective (LES) model. Whilst this method can give clear results on conditions for symmetry-breaking, the difficulty of analysing such large matrices makes the method of limited practical use.

Laurent et al. (2022) consider generalisations of Frank's model to large system sizes, and claim that as the system size increases, the transition to homochiral state becomes

much more likely. This reasoning is based on random matrix theory and assumes the interaction network is sparse.

## Early Experimental Work

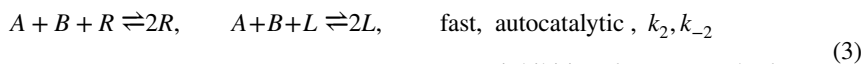
The importance of the chemical production of chiral products has been recognised by several Nobel prizes: from the 2001 awards to Sharpless, Knowles and Noyori for work on chirally catalysed reactions to the recent awards (2021) to List and MacMillan for organo-catalysis. Here, a catalyst accelerates the production of one enantiomer but not the other, resulting in an increase in *ee*.

A similar example is given by Soai et al. (1995) who amplified a small initial enantiomeric excess in a chiral molecule (2%) to 90% by asymmetric autocatalysis (using diisopropylzinc and pyrimidine-5-carboxaldehyde, the original chiral molecule being 5-pyrimidyl alkanol). The catalytic step is the production of more alkanol which is enantioselective.

Girard and Kagan 1998 explore how nonlinear effects can amplify the *ee* of a product relative to initial reagents, and how this reveals the mechanisms that give rise to such nonlinearities. As well as examples of autocatalytic systems taken from organic chemistry, they consider a variety of specific chemical reactions including Metal-Ligand systems, the Diels-Alder reaction, Meerwein-Ponndorf-Verley Reduction - which makes use of a chiral catalyst - so cannot be used to investigate spontaneous symmetry-breaking, which is our focus here.

## Early Theoretical Models

The history of mathematical models of chiral symmetry-breaking chemical processes traditionally start with the system proposed by Frank (1953). This system is 'open' in that a continuous introduction of mass into the system and the continual removal of products from the system are both required in order to maintain an asymmetric state. The processes is summarized by



Here, cross-inhibition ( $k_3$ ) removes equal numbers from  $R$  and  $L$ , which amplifies and maintain differences between the concentrations  $R$ ,  $L$ . Using Eq. (1) we obtain

$$\frac{d(ee)}{dt} = -\frac{1}{2}(R+L)(ee) \left[ (k_{-2} - k_3 + \frac{4k_1AB}{(R+L)^2}) + (ee)^2(k_3 - k_{-2}) \right]. \quad (4)$$

which shows that  $ee = 0$  is stable for small  $k_3$ , and unstable for larger  $k_3$ , undergoing a pitchfork bifurcation which leads to the creation of two stable steady-states at

$$ee = \pm \sqrt{1 - \frac{4k_1AB}{(R+L)^2(k_3 - k_{-2})}}. \quad (5)$$

Saito and Hyuga (2013) propose that, in general, recycling of matter, together with nonlinear processes can drive a system away from a symmetric steady-state and that with input of energy into the system may lead to an asymmetric state with higher energy. This recycling means the resulting system can be ‘closed’, so that no source of fresh material is needed (the input of  $A$ ,  $B$  required in the open system Eq. (2) and no removal terms are required either ( $P \rightarrow \phi$  in Eq. (2)). Saito and Hyuga (2004) discuss how autocatalysis and recycling help achieve homochirality. The nonlinearity induced by autocatalysis amplifies ee, and the authors also suggest that the inclusion of reverse reactions, rather than hindering homochiralisation, may accelerate homochiralisation since it allows material to be recycled to form more of the dominant enantiomer. They consider autocatalytic chemical reactions of the form  $A + B \rightarrow R$  and  $A + B \rightarrow L$ . They assume a closed system with linear degradation at rate  $\lambda$  so that

$$\frac{dR}{dt} = kR^p(1 - R - L) - \lambda R, \quad \frac{dL}{dt} = kL^p(1 - R - L) - \lambda L. \quad (6)$$

In the noncatalytic case  $p = 0$ , they find that the absolute ee  $R - L$  is constant when  $\lambda = 0$ . In the case of linearly autocatalysis ( $p = 1$ ), the relative enantiomeric excess  $ee = \frac{R-L}{R+L}$  is constant when  $\lambda = 0$ . When  $p = 2$  amplification of the ee is again obtained – both when  $\lambda = 0$  and  $\lambda > 0$ .

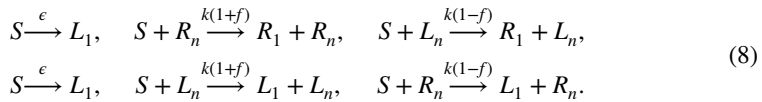
A model allowing achiral monomers coagulate to form chiral clusters from dimers ( $L_2, R_2$ ) to hexamers ( $L_6, R_6$ ) was studied by Saito and Hyuga (2005). Their system had the form

$$\begin{aligned} \frac{dR_2}{dt} &= k_1A^2 - k_2R_2A - \lambda R_2 - 2\mu R_2^2 + 3\nu R_6, & \frac{dR_3}{dt} &= k_2R_2A - k_3R_3A, \\ \frac{dR_4}{dt} &= k_3R_3A - k_4R_4A + \mu R_2^2, & \frac{dR_5}{dt} &= k_4R_4A - k_5R_5A, \\ \frac{dR_6}{dt} &= k_5R_5A - \nu R_6, \end{aligned} \quad (7)$$

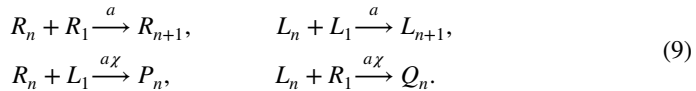
with  $\rho = A + \sum_{i=2}^6 iL_i + iR_i$  being constant, and equations for  $L_i$  being generated by  $L_i \leftrightarrow R_i$  in the above. This allows hexamers to split into dimers and the coagulation of two dimers into a tetramer. They found chiral symmetry breaking even with dimers dissociating to achiral monomers (at rate  $\lambda > 0$ ). However, there is little justification for neglecting other reactions, for example,  $R_4 + R_2 \rightarrow R_6$ ,  $R_4 \rightarrow 2R_2$ ,  $R_3 + R_2 \rightarrow R_5$ ,  $R_6 \rightarrow R_5 + R_1$ ,  $R_5 \rightarrow R_4 + R_1$ ,  $R_4 \rightarrow R_3 + R_1$ , some of which may hinder or prevent symmetry-breaking. Although the scheme Eq. (7) includes some breakdown of larger clusters into smaller ones, it does not satisfy a detailed balancing criteria due to the presence of irreversible reactions. Whilst this lack of detailed balancing allows symmetry-breaking steady-states to be maintained, it means that such states are not equilibria.

## Sandars

In (2003) Sandars used a toy polymerization model to study the formation of chiral structures due to two main processes: enantiomeric cross-inhibition and chiral feedback. The toy model comprises a slow production of chiral monomers ( $L_1, R_1$ ) from a substrate ( $S$ ) together with a faster production due to catalysis by chiral polymers ( $L_n, R_n$  for  $n \geq 2$ ). This step is subject to a fidelity parameter ( $f$ ) which allows  $R_n$  to catalyse the production of  $L_1$  and vice versa. Thus we have



As well as the irreversible growth of homochiral polymers ( $L_n, R_n$ ), the model allows the “poisoning” of homochiral polymers through the addition of a monomer of the opposite chirality. The heteropolymers so produced ( $P_n, Q_n$ ) are do not grow any further. We describe the homochiral and heterochiral polymerisation reactions with corresponding rates by



The resulting system is “open” in terms of mass flux, as it requires a constant input of substrate  $S$ , and the removal of heteropolymers  $P_n, Q_n$ . Solving this system numerically, Sandars found spontaneous symmetry-breaking for sufficiently large fidelity,  $f$ . Sandars compared how the bifurcation depended on the maximum polymer length,  $N$ , finding that the bifurcation occurs more easily at larger  $N$ . According to Sandars, whilst the final polymer product influencing the monomer production is vital to achieving symmetry-breaking, it is not necessary that this is perfect, even highly significant infidelities in the system still allow symmetry-breaking to occur.

Brandenburg et al. (2005) consider Sandars’ model with long polymer chains, demonstrating that the approach to an asymmetric steady-state can occur through “waves” of enhanced chirality moving through the system to polymers of increasing length. They then consider simplified models, and propose the two-ODE system

$$\begin{aligned}
 \frac{dL}{dt} &= \frac{(1+f)L^2(R+\lambda L) + (1-f)R^2(L+\lambda R) + 4C(R+\lambda L)(L+\lambda R)}{2L^2(R+\lambda L) + 2R^2(L+\lambda R) + 8C(R+\lambda L)(L+\lambda R)} - L(L+\lambda R), \\
 \frac{dR}{dt} &= \frac{(1+f)R^2(L+\lambda R) + (1-f)L^2(R+\lambda L) + 4C(R+\lambda L)(L+\lambda R)}{2^2(R+\lambda L) + 2R^2(L+\lambda R) + 8C(R+\lambda L)(L+\lambda R)} - R(R+\lambda L),
 \end{aligned}
 \tag{10}$$

which exhibits similar properties to the full system. In particular, in the special case  $\lambda = 1$ , the symmetric state  $L = R$  is stable when  $f \leq 4C + \frac{1}{2}$ , and when  $f > 4C + \frac{1}{2}$ , there are asymmetric steady-states  $L, R = \frac{1}{2}(1 \pm \sqrt{2f - 1 - 8C})$ .

Wattis and Coveney (2005a) extended the model system Eqs. (8) and (9) to allow infinitely long polymers, which enabled a fully theoretical treatment of the equations. The chirality parameter ( $ee$ ) is then seen to undergo a pitchfork bifurcation, with  $ee = 0$  being stable for smaller values of the fidelity parameter,  $f$ , and becoming unstable for larger values. The critical value of  $f$  varies between  $f_c = 2/9$  (when  $\chi$  is large) to  $f_c = 4/5$ . Another result of the theoretical approach is that the  $ee$  of the monomers makes a relatively slow transition between  $ee = 0$  for  $f < f_c$  and  $ee = \pm 1$  as  $f$  increases. However, the  $ee$  of longer polymers makes a very rapid transition from  $ee = 0$  to  $ee \approx \pm 1$ . This indicates the value of specifying *separate*  $ee$ -parameters for each different species in the system, rather than trying to define a single  $ee$  parameter for the whole system.

Gleiser and Walker (2008) consider a modified Sandars’ model, truncated at various sizes,  $N$ . To simplify the system, they consider an adiabatic approximation, assuming the monomer concentrations rapidly reach a pseudo-steady-state. They find a “phase transition” from stable racemic state at low fidelities to homochiral state at higher fidelities. They find qualitatively similar behaviour for different truncation sizes ( $N$ ), although the position

of transition points changes with system size,  $N$ . They then consider a spatially extended model, and use numerical simulations to illustrate the evolution from almost racemic initial conditions. Their results show the development of homochiral domains, separated by narrow “walls” with smaller domains “dissolving” and walls moving over a slower timescale.

Various stochastic models of based on Sandars model are simulated using Monte-Carlo techniques by Brandenburg (2019). His aim is to investigate the effect of fluctuations on homochiralization dynamics; he finds symmetry-breaking in most cases, although it can take up to a billion reaction steps to achieve when 30,000 molecules are involved. Another study making use of large simulations has been performed by Konstantinov and Konstantinova (2020) who generalise Sandars’ model to describe and simulate chiral symmetry-breaking in large peptide systems. Their approach is to simulate a large system of ODEs (65K variables) describing monomers, dimers and trimers, where each monomer could be one of 20 amino acids. They found symmetry-breaking in a significant number of cases.

## Chiral Crystallisation Experiments

In (1998), Kipping and Pope (1898a, b) observed the crystallization of sodium chlorate ( $\text{NaClO}_3$ ), via spontaneous (primary) nucleation, as well as with seeding (secondary nucleation). For each sample observed, the ratio of  $L$  and  $R$  crystals was recorded. After repeating the experiment several times, the authors concluded that homochiral sodium chlorate crystals could be produced through saturated solutions, with adequate seeding.

Kondepudi et al. (1990) investigated the effect of *stirring* on the growth of sodium chlorate crystals from a supersaturated solution, finding that crystals obtained from unstirred solutions had roughly equal numbers of right-hand and left-handed crystals. However, solutions that were stirred during crystallization, yielded most (99.7%) crystals of the same chirality; that is, almost all right-handed or almost all left-handed. The authors attributed their results to a combination of autocatalysis and competition between  $L$  and  $R$  crystals. The reason for autocatalysis is that, when stirred, most crystallization is due to secondary nucleation - that is, birth from a ‘mother crystal’; and if that ‘mother crystal’ arose from secondary nucleation, then there was a ‘grandmother’ crystal; hence, using biological terminology in homochiral systems, all the crystals of the same handedness could be described as coming from a (last) ‘universal common ancestor’ (LUCA).

The solidification of sodium chlorate was filmed by McBride and Carter (1991) who observed that the first nucleated crystal broke into small fragments, which later acted as secondary nucleation centers. This favoring the growth of new crystals of the same handedness, and caused a subsequent rapid decrease in supersaturation which repressed primary nucleation.

## Viedma Grinding

The recrystallisation process of sodium chlorate was investigated by Viedma (2005). In these experiments, an initially racemic mixture of crystals was stirred - so there is no LUCA. The stirring caused a continual fragmentation, however, the supersaturation of the solution was maintained, so in a single system there is crystals growth occurring at the same time as dissolution. After a few hours, chiral symmetry-breaking was observed, as all crystals in the reactor eventually exhibited the same chirality. This now-famous method is known as Viedma grinding or Viedma deracemization. Homochirality is achieved through autocatalytic recycling.

Noorduyn et al. (2008) showed that this mechanism of deracemization could be successfully applied to chiral crystals of amino acids, increasing the interest in the origins of life community. Although the deracemisation process took a long time (10 days), the *ee* increased exponentially during the process.

The Nature review of McBride and Tully (2008) discussed Viedma's work (2005), suggesting that, in addition to Oswald ripening (where larger crystals grow at the expense of smaller crystals), complete deracemization could be achieved through a molecular recognition step. Many solids can adopt two mirror-image crystal forms and often grow as mixtures of both. Whilst grinding hinders the growth of the larger crystals, this may not be a hindrance to homochiralisation if the fragments are able to reabsorb onto crystals of the same handedness without needing to undergo dissolution.

Later, Viedma and Cintas (2011) analysed chiral symmetry-breaking by a temperature gradient as a solution is heated. They showed that a single-chirality solid phase can be obtained by boiling solutions that initially contain a racemic mixture of left and right enantiomorphs. Repeated dissolution-crystallization cycles induced by a temperature gradient results in amplification of *ee* via other mechanisms which are relevant to the origins of life. Hydrothermal vents and hot springs (both produced by geothermal heating) provide scenarios of prebiotic interest. Viedma and Cintas (2011) also point out that controlled boiling may be harnessed for the production of chiral compounds of pharmaceutical or industrial interest.

Tsogoeva et al. (2009) also observed the formation of chiral crystals of organic molecules. This was the result of the Mannich reaction, which combines three reagents and results in a chiral product which forms chiral conglomerates. The authors concluded that the combination of stirring (with or without grinding) of pre-formed crystalline conglomerates of chiral products with low *ee* may provide a good method for obtaining products with a high *ee* (up to 100 %).

## Mathematical Models

A simple physical crystallization model has been presented by Uwaha (2004) who proposes that homochiral crystals are formed from achiral molecules. The system of differential equations proposed has five components: achiral molecules ( $Z$ ), which combine at rate  $k_0$  to form right- and left-handed chiral units (nuclei, denoted by  $R_u$  and  $L_u$ , respectively). These chiral units combine with each other to form larger chiral crystals ( $R$ ,  $L$ ) at rate  $k_c$ . In addition, small and large crystals of the same chirality combine at rate  $k_u$  to form more larger crystals, and at rate  $k_1$  monomers combine with large crystals to form more larger crystals. This includes fragmentation of small and larger crystals, at rates  $\lambda_0$ ,  $\lambda_1$  respectively. This recycling of the materials through the decay processes is essential in attaining the complete homochirality. The model can be written as

$$\frac{dZ}{dt} = -2k_0Z^2 - k_1Z(R+L) + \lambda_1(R+L) + \lambda_0(R_u+L_u), \quad (11)$$

$$\frac{dR_u}{dt} = k_0Z^2 - k_uR_uR - k_cR_u^2 + \lambda_uR - \lambda_0R_u, \quad (12)$$

$$\frac{dL_u}{dt} = k_0Z^2 - k_uL_uL - k_cL_u^2 + \lambda_uL - \lambda_0L_u, \quad (13)$$



$$\frac{dR}{dt} = k_1 ZR + k_u R_u R + k_c R_u^2 - \lambda_1 R - \lambda_u R, \tag{14}$$

$$\frac{dL}{dt} = k_1 ZL + k_u L_u L + k_c L_u^2 - \lambda_1 L - \lambda_u L. \tag{15}$$

Uwaha notes that autocatalysis arises from the reaction of chiral units so that chiral asymmetry is amplified as crystallization proceeds, and that homochirality is achieved through slow relaxation at a later stage of crystallization. The only form of aggregation that is not included in the model is the combination of monomers ( $Z$ ) with small crystal nuclei ( $L_u, R_u$ ); this model also neglects the fragmentation of larger crystals into smaller crystals, neither does it have a conserved quantity corresponding to total mass or density of the system. We also note that, whilst the model exhibits symmetry-breaking, having an unstable symmetric steady-state and stable asymmetric steady-states, these should not be described as thermodynamic equilibria, since the fundamental processes modelled are irreversible, a property shared with the models Eqs. (8) and (9) of Sandars (2003), and Eqs. (6)–(7) from Saito and Hyuga (2004) and (2005).

Similar phenomena are exhibited by a more complicated model of grinding proposed by Wattis (2010), where the range of cluster sizes is extended using a modified Becker-Döring model (Becker and Döring 1935). This model allows step-wise cluster growth as in classical nucleation theory, that is, the addition or removal of a single achiral monomer ( $C_1$ ) at a time with rates  $a_n, b_n$ ; in addition, the model allows the growth and fragmentation of chiral clusters ( $L_n, R_n$ ) by the addition or removal of small chiral fragments ( $L_2, R_2$ ) with rates  $\xi, \beta$ . These small fragments are also permitted to change chirality via an intermediate achiral fragment  $C_2$  (rates  $\mu, \mu\nu$ ). The achiral fragment  $C_2$  is formed (reversibly) from achiral monomers at rates  $\delta, \epsilon$ ;  $C_2$  can also combine with larger chiral nuclei at rate  $\alpha_n$ . Thus the model can be written as

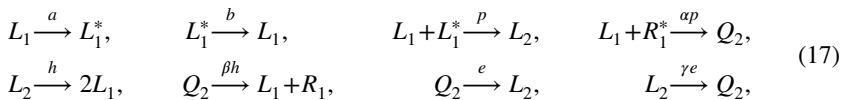
$$\begin{aligned} \frac{dL_n}{dt} &= a_{n-1}C_1L_{n-1} - a_nC_1L_n - b_nL_n + b_{n+1}L_{n+1} + \alpha_{n-2}C_2L_{n-2} \\ &\quad - \alpha_nC_2L_n - \beta_nL_n + \beta_{n+2}L_{n+2} + \xi_{n-2}L_2L_{n-2} - \xi_nL_n, \\ \frac{dL_3}{dt} &= a_2C_1L_2 - a_3C_1L_3 - b_3L_3 + b_4L_4 - \alpha_3C_2L_3 - \xi_3L_2L_3 + \beta_5L_5, \\ \frac{dL_2}{dt} &= \mu(C_2 - \nu L_2) - a_2C_1L_2 + b_3L_3 - \alpha_2C_2L_2 + \beta_4L_4 - \xi L_2^2 \\ &\quad - \sum_{n=2}^{\infty} (\xi_n L_2 L_n - \beta_{n+2} L_{n+2}), \\ \frac{dC_2}{dt} &= \mu(\nu R_2 + \nu L_2 - 2C_2) + \delta C_1^2 - \epsilon C_2 - C_2 \sum_{n=2}^{\infty} \alpha_n (R_n + L_n), \\ \frac{dC_1}{dt} &= 2\epsilon C_2 - 2\delta C_1^2 - \sum_{n=2}^{\infty} (a_n C_1 L_n + a_n C_1 R_n - b_{n+1} L_{n+1} - b_{n+1} R_{n+1}), \end{aligned} \tag{16}$$

with similar equations for  $R_n, R_3, R_2$  obtained by symmetry ( $R_n \leftrightarrow L_n$ ). Since energy is continually supplied to maintain the fragmentation, there is no requirement for the rate coefficients to satisfy a detailed balancing condition. This model has a conserved quantity,  $\rho = C_1 + 2C_2 + \sum_n n(L_n + R_n)$ .

Blanco et al. (2017) model the grinding experiments of Viedma using a model of homochiral growth of clusters from chiral monomers, chirality of monomers can flip, but the handedness of larger clusters cannot be changed without disintegration to monomers and re-aggregation. The model includes two mixed Becker-Döring and Smoluchowski coagulation-fragmentation systems operating at different (but overlapping) cluster sizes, which are coupled through monomers which can flip chiralities. Their numerical results show  $ee$  increasing to totality ( $\pm 1$ ) over extremely long timescales.

## The APED Model

The model proposed in 2004 by Plasson et al. (2004), describes a dynamic chemical system of reacting chiral monomers, composed of activation, polymerization, epimerization, and depolymerization (APED) reactions between unactivated monomers ( $L_1$  and  $R_1$ ), activated monomers ( $L_1^*$  and  $R_1^*$ ), and polymers. For simplicity, the authors limited polymerization reactions to dimers, that is, reactions involving a pair of monomers whose product is the formation of polymers of length two. Homopolymers  $L_2 = L_1L_1, R_2 = R_1R_1$  are formed by the combining of an activated and an unactivated monomer of the same handedness, which occurs at rate  $p$ . The two forms of heteropolymers form from combinations of monomers of opposite chiralities, and this is assumed to occur at the rate  $\alpha p$ ; note that  $Q_2 = L_1R_1$  is treated as a distinct species from  $P_2 = R_1L_1$ . Depolymerisation results in the splitting of a polymer into its unactivated monomers; this occurs at the rate  $h$  for homopolymers, and  $\beta h$  for heteropolymers. Unactivated monomers become activated at a rate  $a$ , and activated monomers relax to unactivated at the rate  $b$ . Thus we have



together with the mirror image reactions obtained by swapping  $L$  and  $R$  in every reaction. We note that  $\alpha, \beta, \gamma$  are nondimensional parameters,  $h, e, a, b$  have units of  $[T]^{-1}$  whilst  $p$  has units of  $[conc]^{-1}[T]^{-1}$ . Whilst the activation/deactivation and polymerisation/depolymerisation reactions are commonplace and well-studied, the effect of epimerisation, and its interaction with the other processes is the major novel aspect of this work.

Since the full set of reactions is challenging to analyze, Plasson et al. (2004) formulated a simplified case where the depolymerization and epimerization reactions were fully stereospecific ( $\beta = \gamma = 0$ ). They then analysed the effects of just the stereospecificity of the polymerization reaction ( $\alpha$ ), and the mass in the system. They found that the system evolves into one of four types of behaviour:

- (i) a 'dead' state for small mass and small  $\alpha$ , in which there are few dimers, most of the mass remains in monomeric form ( $R_2, L_2, Q_2, P_2 \ll 1$ );
- (ii) an asymmetric steady-state for large mass and small  $\alpha$ , in which  $L_2 \neq R_2, P_2 \neq Q_2, R_1 \neq L_1$  and  $R_1^* \neq L_1^*$ ;
- (iii) a symmetric steady-state for moderate  $\alpha$  and moderate-large mass, in which there are significant numbers of dimers, but  $R_2 = L_2$  and  $P_2 = Q_2, L_1 = R_1$  and  $R_1^* = L_1^*$ ;
- (iv) an unstable state (where the chirality oscillates), here there is significant numbers of dimers but the concentrations  $L_2, R_2$  oscillate out of phase with each other, so the system continuously changes from left-dominated to right and back again.

Brandenburg et al. (2008) consider modified APED model, with  $L_1 \leftrightarrow R_1$  (at rate  $r$ ) and no de-activation of  $R_1^*, L_1^* \rightarrow R_1, L_1$  (i.e.  $b = 0$ ). Whilst one may expect this racemisation reaction to hinder the growth of homochiral structures, they still find homochiral behaviour for small values of  $r$  and  $0 < \alpha < 1$ . They discuss the role of epimerisation in causing spontaneous symmetry-breaking in APED models and show correspondances with autocatalysis and mutual inhibition in other symmetry-breaking models.

Stich et al. (2013) consider the dimeric APED model, and investigate oscillatory solutions using numerical bifurcation methods. They find sustained oscillations for large  $\alpha$  and intermediate values of total mass. They note that oscillations cease to exist at very large and very small masses. Their initial work focuses on the case  $b = \beta = \gamma = 0$  and  $a = h = e = p = 1$ , although they later investigate  $\beta, \gamma$  nonzero and find that only for small values of  $\beta, \gamma$  do oscillations persist; and then also only for smaller values of  $e, h$ .

Danger et al. (2010) present the results of experiments on chiral peptides which involves trimers as well as dimers. They find that homopolymer dimers are outnumbered by heteropolymeric dimers, but upon the extension to trimers, homopolymers become more stable. They observe epimerisation and postulate different growth rates for homopolymers and heteropolymers. This helps establish that the mechanisms in the APED model may be relevant to more complex chemicals relevant to the origins of life.

Bock and Peacock-Lopez (2020) also expand the APED model to include trimers and perform numerical simulations, finding oscillations in the enantiomeric excess. They also performs numerical path-following of solutions in parameter space to identify the locations of bifurcations, finding classic pitchfork and Hopf diagrams. They further extend the models to tetramers and pentamers, and note that the period of oscillation increases with system size.

Gleiser and Walker (2009) have simulated a spatially extended version of the dimer APED system, where the species move by diffusion, in addition to undergoing the usual APED reactions. Simulations starting with stochastic initial conditions are then observed to form domains where left-handed and right-handed species dominate, and the global average  $ee$  grows slowly and steadily away from zero. A range of spatial patterns are found to form, from small 'islands' of one chirality surrounded by the other, to larger domains, as the system evolves to a single chirality, with the intermediate dynamics governed by the motion of thin racemic 'walls' which divide left-dominated and right-dominated regions. For some parameter values, they also note the relative stability of small 'chiral protocell-like regions'.

Whilst APED models are 'closed' in the sense that mass is conserved in the system, and there is no introduction or removal of any material, they are not 'closed' in energetic terms. The activation of monomers typically requires energy and there is no balance of energy input/output when monomers are released due to fragmentation. There is also no detailed balancing (the system is modelled by a combination of irreversible reactions). Hence, there is no requirement for the system to satisfy the basic laws of Thermodynamics. These issues are discussed further by Plasson (2008) and Blackmond (2008).

Montoya et al. (2019) analyse general network models of complex chemical reactions, and derive general rules for the stability and instability of the symmetric state which can be used to determine when symmetry-breaking occurs. These rules are then illustrated on a range of systems, including the dimeric APED system. Whilst the method makes clear distinctions between parameter regions of stability and instability of the symmetric state, it does not appear to make clear distinctions between pitchfork and Hopf bifurcations.

## Adiabatic Approximations in APED

In this section we summarise some new results obtained by taking two different adiabatic approximations of the APED system. The expected concentrations given by the reactions Eq. (17) are described by the ordinary differential equations

$$\begin{aligned}
 \frac{dL_1}{dt} &= (-a - pL_1^* - \alpha pR_1^*)L_1 + bL_1^* + \beta h(Q_2 + P_2) + 2hL_2, \\
 \frac{dL_1^*}{dt} &= aL_1 - (b + pL_1 + \alpha pR_1)L_1^*, \\
 \frac{dL_2}{dt} &= pL_1^*L_1 + eQ_2 - (\gamma e + h)L_2, \\
 \frac{dQ_2}{dt} &= \alpha pL_1R_1^* + \gamma eL_2 - (\beta h + e)Q_2, \\
 \frac{dR_1}{dt} &= (-a - pR_1^* - \alpha pL_1^*)R_1 + bR_1^* + \beta h(P_2 + Q_2) + 2hR_2, \\
 \frac{dR_1^*}{dt} &= aR_1 - (b + pR_1 + \alpha pL_1)R_1^*, \\
 \frac{dR_2}{dt} &= pR_1^*R_1 + eP_2 - (\gamma e + h)R_2, \\
 \frac{dP_2}{dt} &= \alpha pR_1L_1^* + \gamma eR_2 - (\beta h + e)P_2.
 \end{aligned} \tag{18}$$

We note that  $P_2$  and  $Q_2$  are distinct since we assume polymers are directional, that is, as noted earlier,  $Q_2 = L_1R_1$  is distinct from  $P_2 = R_1L_1$ .

Following earlier comments, we define chiralities (or  $ee$ 's) for each chemical species, and corresponding total concentrations for each species, which are given by

$$\mu = \frac{R_1 - L_1}{R_1 + L_1}, \quad \delta = \frac{R_2 - L_2}{R_2 + L_2}, \quad \chi = \frac{R_1^* - L_1^*}{R_1^* + L_1^*}, \quad \rho = \frac{P_2 - Q_2}{P_2 + Q_2}, \tag{19}$$

$$M = R_1 + L_1, \quad A = R_1^* + L_1^*, \quad D = R_2 + L_2, \quad S = P_2 + Q_2. \tag{20}$$

which are equivalent to

$$\begin{aligned}
 R_1 &= \frac{1}{2}M(1 + \mu), & R_1^* &= \frac{1}{2}A(1 + \chi), & R_2 &= \frac{1}{2}D(1 + \delta), & P_2 &= \frac{1}{2}S(1 + \rho), \\
 L_1 &= \frac{1}{2}M(1 - \mu), & L_1^* &= \frac{1}{2}A(1 - \chi), & L_2 &= \frac{1}{2}D(1 - \delta), & Q_2 &= \frac{1}{2}S(1 - \rho).
 \end{aligned} \tag{21}$$

The racemic state corresponds to the case where all  $ee$ 's are zero, that is, all the chiralities  $\mu = \delta = \chi = \rho = 0$ . The total concentrations evolve according to

$$\begin{aligned}
 \frac{dM}{dt} &= -aM - \frac{1}{2}pAM(1 + \chi\mu) - \frac{1}{2}\alpha pAM(1 - \chi\mu) \\
 &\quad + bA + 2\beta hS + 2hD, \\
 \frac{dA}{dt} &= aM - bA - \frac{1}{2}pAM(1 + \chi\mu) - \frac{1}{2}\alpha pAM(1 - \chi\mu), \\
 \frac{dD}{dt} &= \frac{1}{2}pAM(1 + \chi\mu) + eS - \gamma eD - hD, \\
 \frac{dS}{dt} &= \frac{1}{2}\alpha pAM(1 - \chi\mu) - eS + \gamma eD - \beta hS,
 \end{aligned}
 \tag{22}$$

which, at steady-state, and in the racemic state, are solved by

$$A = \frac{2aM}{2b + pM(1 + \alpha)}, \quad D = \frac{paM^2B_D}{2b + pM(1 + \alpha)}, \quad S = \frac{paM^2B_S}{2b + pM(1 + \alpha)} \tag{23}$$

where  $B_D, B_S$  are given by

$$B_D = \frac{\alpha e + e + \beta h}{h(e + \beta h + \beta \gamma e)}, \quad B_S = \frac{\gamma e + \alpha h + \alpha \gamma e}{h(e + \beta h + \beta \gamma e)}. \tag{24}$$

If all chiralities are zero ( $\mu = \chi = \rho = \delta = 0$ ), they remain zero, but if one or more deviate away from zero, they evolve according to

$$\frac{d\mu}{dt} = \frac{1}{2}pA\chi(\mu^2 - 1)(1 - \alpha) + \frac{bA}{M}(\chi - \mu) - \frac{2\beta hS\mu}{M} + \frac{2hD}{M}(\delta - \mu), \tag{25}$$

$$\frac{d\delta}{dt} = \frac{pAM}{2D}(\chi + \mu - \delta - \delta\chi\mu) + \frac{eS}{D}(\rho - \delta), \tag{26}$$

$$\frac{d\chi}{dt} = \frac{aM}{A}(\mu - \chi) + \frac{1}{2}pM\mu(\chi^2 - 1) + \frac{1}{2}p\alpha M\mu(1 - \chi^2), \tag{27}$$

$$\frac{d\rho}{dt} = -\frac{\alpha pAM}{2S}(\chi - \mu + \rho - \rho\chi\mu) + \frac{\gamma eD}{S}(\delta - \rho). \tag{28}$$

Here, we aim to investigate the stability of the racemic state, that is, we want to know the stability of the state  $\mu = \delta = \chi = \rho = 0$ . Hence we investigate the dynamics of these quantities when they are small. When all the chiralities are small, we can linearise, giving the linear system

$$\frac{d}{dt} \begin{pmatrix} \mu \\ \delta \\ \chi \\ \rho \end{pmatrix} = \begin{pmatrix} \frac{bA}{M} - \frac{2h(\beta S + D)}{M} & \frac{2hD}{M} & \frac{pA}{2}(\alpha - 1) + \frac{bA}{M} & 0 \\ \frac{pAM}{2D} & -\frac{pAM}{2D} - \frac{eS}{D} & \frac{pAM}{2D} & \frac{eS}{D} \\ \frac{aM}{A} + \frac{pM}{2}(\alpha - 1) & 0 & -\frac{aM}{A} & 0 \\ \frac{\alpha pAM}{2S} & \frac{\gamma eD}{S} & -\frac{\alpha pAM}{2S} & -\frac{\alpha pAM}{2S} - \frac{\gamma eD}{S} \end{pmatrix} \begin{pmatrix} \mu \\ \delta \\ \chi \\ \rho \end{pmatrix}. \tag{29}$$

The stability of the racemic state depends upon the eigenvalues of this linear system ( $\lambda$ ), which are determined by the roots of the characteristic polynomial of this matrix, which we write as

$$\lambda^4 + a_3\lambda^3 + a_2\lambda^2 + a_1\lambda + a_0 = 0. \tag{30}$$

Thus we need to know the signs of the real parts of all the eigenvalues, with positive real parts meaning that the racemic state is unstable. Typically, there will be some parameter values for which all the eigenvalues have negative real parts and so the racemic state is stable.

As we vary one of the parameter values (for example, monomeric mass,  $M$ , or polymerisation rate  $p$ , or one of the chiral fidelities  $\alpha, \beta, \gamma$ ) the eigenvalues  $\lambda$  change. If one crosses from negative to positive through  $\lambda = 0$ , then we expect to see a pitchfork bifurcation, as two new stable steady-states are created (one left-dominated, and the other right-dominated). If a pair of complex conjugate eigenvalues cross from  $\text{Re}(\lambda) < 0$  to  $\text{Re}(\lambda) > 0$ , then we will see a Hopf bifurcation, and a stable periodic orbit is formed, corresponding to the system oscillating between being left-dominated and right-dominated. In general, finding the roots is not straightforward, although the signs can be determined using the Routh-Hurwitz criteria (Murray 1989). In the subsections below, we investigate the conditions for which each of these bifurcations can occur in some special cases, by considering adiabatic approximations, that is, we assume that some processes occur on faster timescales than others, thus we can assume some of the chiralities adapt to a pseudo-steady-state whilst others evolve more slowly.

### First Adiabatic Approximation

Firstly, we will take the large-mass limit ( $M \gg 1$ ), since in the numerical results of Plasson et al. (Fig. 3 of Plasson et al. 2004) this is the region where asymmetric steady-states are found for  $\alpha < 1$  and oscillatory behaviour for very large  $\alpha$  (in the special case of  $\beta = \gamma = b = 0, a = h = e = p = 1$ ). In the case of  $M \gg 1$ , from Eq. (30), we have

$$\begin{aligned} a_0 &:= M\hat{a}_0 \sim \frac{hpa e M}{1 + \alpha} (\alpha^2 - \alpha + \beta\gamma + 3\alpha\beta\gamma), \\ a_1 &:= M\hat{a}_1 \sim \frac{pM}{2(\alpha + 1)} (h(\alpha + 1)^2(e + \beta h + \beta\gamma e) + 2a(1 + 3\alpha)(e + \beta h + \gamma e)), \\ a_2 &:= M\hat{a}_2 \sim \frac{pM}{2(\alpha + 1)} ((\alpha + 1)^2(e + h + \beta h + \gamma e) + 2a(1 + 3\alpha)), \end{aligned} \tag{31}$$

$$a_3 := M\hat{a}_3 \sim \frac{1}{2} pM(1 + \alpha). \tag{32}$$

The characteristic polynomial is

$$0 = \lambda^4 + M(\hat{a}_3\lambda^3 + \hat{a}_2\lambda^2 + \hat{a}_1\lambda + \hat{a}_0), \tag{33}$$

and there is one large negative eigenvalue,

$$\lambda_4 = M\hat{\lambda}_4 \sim -M\hat{a}_3 \sim -\frac{1}{2} pM(1 + \alpha), \tag{34}$$

which has the corresponding eigenvector  $(0, 0, 1, 0)^T$ . This means that the chirality  $\chi(t)$  of the activated monomers ( $R_1^*, L_1^*$ ) equilibrates much more rapidly than the other species.

From Eq. (29), the linear equation for  $\chi$  is

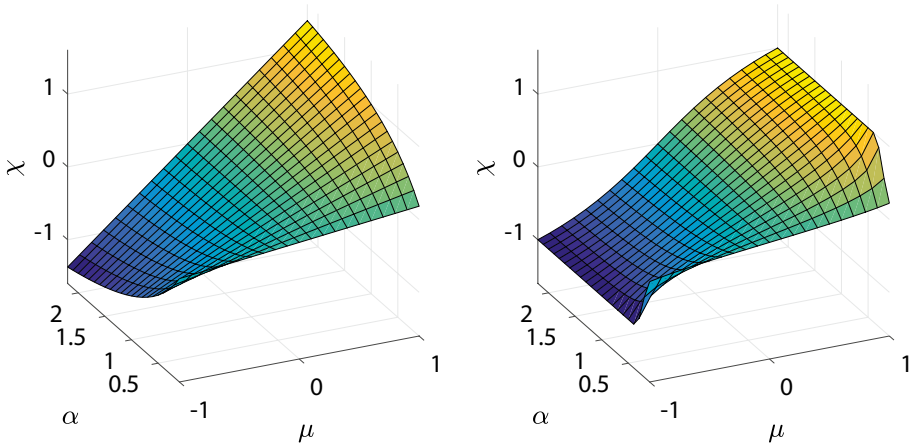


**Fig. 1** Illustration of linear Eq. (36), on the left, and nonlinear Eq. (37), on the right, adiabatic approximations to the chirality of activated monomers  $\chi$  as a function of unactivated monomers  $\mu$  and relative heteropolymerisation rate  $\alpha$ . In colour in online version

$$\frac{d\chi}{dt} = \left( \frac{aM}{A} + \frac{pM(\alpha - 1)}{2} \right) \mu - \frac{aM\chi}{A}. \tag{35}$$

Since  $\chi$  evolves on a fast timescale, we could assume that  $\chi$  takes the pseudo-steady-state value  $\chi = \chi(\mu)$  given by

$$\begin{aligned} \chi &= \mu \left( \frac{aM}{A} + \frac{1}{2} pM(\alpha - 1) \right) \frac{A}{aM} = \mu \left( 1 + \frac{1}{2} pAa^{-1}(\alpha - 1) \right) \\ &= \frac{2\alpha\mu}{\alpha + 1}. \end{aligned} \tag{36}$$

Then we use this formula for  $\chi$  as  $\delta, \mu, \rho$  evolve according to the other equations on a slower timescale. More generally, we could return to the nonlinear equation for  $\chi$  Eq. (27) and find a more accurate expression for  $\chi$ , namely

$$\chi = \frac{4\alpha\mu}{1 + \alpha + \sqrt{(1 + \alpha)^2 - 8\alpha\mu^2(1 - \alpha)}}. \tag{37}$$

This formula is preferable, since it satisfies  $|\chi| \leq 1$ , whereas Eq. (36) allows unphysical values of  $|\chi| \geq 1$  if  $\alpha$  and  $\mu$  were both large. Note that for small  $\mu$ , the two formulae Eqs. (36) and (37) agree. Both the formulae (36) and (37) are plotted in Fig. 1.

Returning to Eq. (33), three eigenvalues remain to be considered, assuming that these are  $\mathcal{O}(1)$ , they are determined by

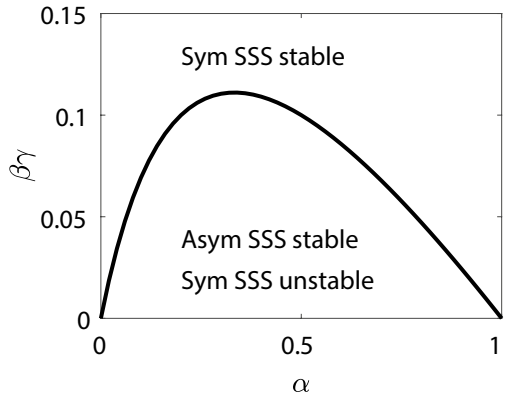
$$0 = \hat{a}_3\lambda^3 + \hat{a}_2\lambda^2 + \hat{a}_1\lambda + \hat{a}_0. \tag{38}$$

For a pitchfork bifurcation to occur, we need  $\hat{a}_0 = 0$ , which, from Eq. (31), implies

$$\beta\gamma = \Gamma_c(\alpha) := \frac{\alpha(1 - \alpha)}{1 + 3\alpha}. \tag{39}$$

If  $a_0 > 0$  then the zero chirality state is stable, we only find an instability if  $a_0 < 0$ , which corresponds to the case  $\beta\gamma < \Gamma_c(\alpha)$ . In Fig. 2, we show the curve  $\beta\gamma = \Gamma_c(\alpha)$ , and

**Fig. 2** Illustration of the location of the pitchfork bifurcation in  $(\alpha, \beta\gamma)$  space. Asymmetric steady-state solutions (SSS) gain stability in the region below the curve (the symmetric steady-state solution still exists below the curve, but is unstable), whereas above the curve, only the symmetric steady-state solution exists and it is stable there



identify the area below the curve as the region where we expect to find asymmetric steady-states in the case of large mass  $M$ .

Alternatively, from Eq. (31), if we consider  $\alpha$  as the bifurcation parameter, we find asymmetric steady-states when

$$\begin{aligned} \frac{1}{2}(1 - 3\beta\gamma) - \frac{1}{2}\sqrt{(1 - \beta\gamma)(1 - 9\beta\gamma)} < \alpha \quad \text{and} \\ \alpha < \frac{1}{2}(1 - 3\beta\gamma) + \frac{1}{2}\sqrt{(1 - \beta\gamma)(1 - 9\beta\gamma)}. \end{aligned} \tag{40}$$

This region is illustrated in Fig. 2. This shows that larger values of  $\beta$  and  $\gamma$  are expected to stabilise the racemic state, or allow oscillatory behaviour.

The condition for a Hopf bifurcation to occur is when the cubic Eq. (38) can be written as

$$\hat{a}_3(\lambda^2 + \omega^2)(\lambda + \hat{a}_0\hat{a}_3^{-1}\omega^{-2}), \quad \omega^2 = \frac{\hat{a}_1}{\hat{a}_3} = \frac{a_1}{a_3} > 0. \tag{41}$$

In order for this be satisfied, we need  $\hat{a}_1\hat{a}_2 = \hat{a}_0\hat{a}_3$  (which is equivalent to  $a_1a_2 = a_0a_3$ , giving  $\omega^2 = a_0/a_2$ ). This implies

$$\begin{aligned} 2ae \frac{(\alpha^2 - \alpha + 3\alpha\beta\gamma + \beta\gamma)}{(\alpha + 1)^2} = \left[ e + \beta h + \beta\gamma e + \frac{2a(e + \beta h + \gamma e)(1 + 3\alpha)}{h(1 + \alpha)^2} \right] \times \\ \left[ e + \beta h + h + \gamma e + \frac{2a(1 + 3\alpha)}{(1 + \alpha)^2} \right], \end{aligned} \tag{42}$$

which cannot be satisfied, and so there is no Hopf bifurcation in the case of large mass ( $M \gg 1$ ), with  $a, p, h, b, e, \alpha, \beta, \gamma = \mathcal{O}(1)$ .

### Second Adiabatic Approximation

Since Plasson et al. (2004) found oscillatory behaviour when  $\alpha$  was large, we now consider the large  $\alpha$  limit of the governing equations. We consider  $\alpha \gg 1$  and treat all other parameters as  $\mathcal{O}(1)$ ; this is entirely consistent since  $\alpha$  is a nondimensional parameter. In this case, we return to Eq. (30) and obtain



$$\begin{aligned}
 a_3 &\sim \frac{1}{2}\alpha pM + \mathcal{O}(1), \\
 a_2 &\sim \frac{1}{2}\alpha pM(h + \beta h + e + \gamma e) + \mathcal{O}(1), \\
 a_1 &\sim \frac{1}{2}\alpha pMh(e + \beta h + \beta \gamma e) + \mathcal{O}(1), \\
 a_0 &\sim \alpha pMhea + \mathcal{O}(1).
 \end{aligned}
 \tag{43}$$

since

$$B_D \sim \frac{\alpha e}{h(e + \beta h + \beta \gamma e)}, \quad B_S \sim \frac{\alpha(h + \gamma e)}{h(e + \beta h + \beta \gamma e)},
 \tag{44}$$

$$\mathcal{M} = M + \frac{2aM(e + h + \gamma e)}{h(e + \beta h + \beta \gamma e)} + \mathcal{O}(\alpha^{-1}),
 \tag{45}$$

where  $\mathcal{M} = M + A + 2D + 2S$  is the total mass in the system. To simplify the later analysis, we introduce

$$B = \frac{1}{2}\alpha pM \gg 1,
 \tag{46}$$

then the characteristic polynomial can be written as

$$B^{-1}\lambda^4 + \lambda^3 + (h + e + \beta h + \gamma e)\lambda^2 + h(e + \beta h + \beta \gamma e)\lambda + 2hea = 0,
 \tag{47}$$

which has one large eigenvalue, namely,  $\lambda_4 = -B$ , and the other three are  $\mathcal{O}(1)$ , as with the first adiabatic approximation. Keeping only the first two terms in  $B$ , (namely terms of  $\mathcal{O}(B)$  and  $\mathcal{O}(1)$ ) the Jacobian matrix Eq. (29) can be written as

$$\mathbf{J}_2 = \begin{pmatrix} -2a & \frac{2a}{e+\beta h+\beta \gamma e} & a & 0 \\ 0 & -h - \gamma e & 0 & h + \gamma e \\ 2B & 0 & -B & 0 \\ \frac{h(e+\beta h+\beta \gamma e)}{h+\gamma e} & \frac{\gamma e^2}{h+\gamma e} & \frac{-h(e+\beta h+\beta \gamma e)}{h+\gamma e} & \frac{-\gamma e^2 - h(e+\beta h+\beta \gamma e)}{h+\gamma e} \end{pmatrix}.
 \tag{48}$$

Thus we see that the fast timescale again corresponds to the rapid equilibration of  $\chi$  – the chirality of the activated monomers. We can thus put  $\chi = 2\mu$  if we follow the linear approximation, or, more realistically, let  $\chi$  be the solution of the fully nonlinear equation for  $\chi$ , namely

$$\frac{d\chi}{dt} = B[\mu - \chi + \mu(1 - \chi^2)],
 \tag{49}$$

which implies

$$\chi = \frac{4\mu}{1 + \sqrt{1 + 8\mu^2}}.
 \tag{50}$$

As with the first adiabatic approximation, the nonlinear version is preferred since it satisfies  $|\chi| \leq 1$ .

Returning to Eq. (47), the three  $\mathcal{O}(1)$  eigenvalues are determined by

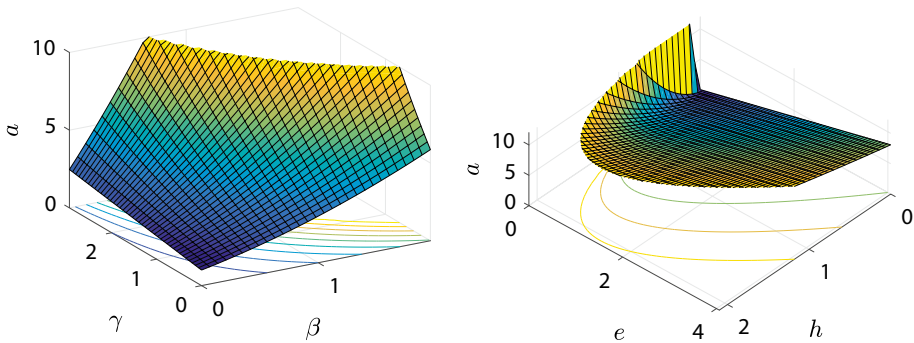


**Fig. 3** Location of Hopf bifurcation in  $(\beta, \gamma, a_c)$ -space (left) with  $e = h = 1$ ; and  $(e, h, a_c)$ -space (right) with  $\beta = \gamma = 1$ ; in both cases, surfaces are given by Eq. (53), with the symmetric-steady-state solution being stable for  $a < a_c$  and there being an oscillatory solution for  $a > a_c$ . (In color in online version)

$$\lambda^3 + (h + e + \beta h + \gamma e)\lambda^2 + h(e + \beta h + \beta \gamma e)\lambda + 2hea = 0. \tag{51}$$

Since  $\lambda = 0$  can never be a solution of this, there is no pitchfork bifurcation, and in this limit, no stable asymmetric steady-state can be formed.

However, in this limit, a Hopf bifurcation is possible. The cubic Eq. (51) can be written as  $(\lambda^2 + \omega^2)(\lambda + K) = 0$ , namely

$$(\lambda^2 + h(e + \beta h + \beta \gamma e))\left(\lambda + \frac{2ea}{e + \beta h + \beta \gamma e}\right) = 0, \tag{52}$$

if

$$a = a_c(e, h, \beta, \gamma) := \frac{(h + e + \beta h + \gamma e)(e + \beta h + \beta \gamma e)}{2e}. \tag{53}$$

In this case

$$\omega = \pm \sqrt{h(e + \beta h + \beta \gamma e)}. \tag{54}$$

The symmetric steady-state solution is stable if  $a < a_c$  and unstable due to the presence of an oscillatory mode if  $a > a_c$ . The surface  $a_c(e, h, \beta, \gamma)$  is plotted in Fig. 3.

In Fig. 4 we present illustrations of the oscillatory solutions in a dimer APED system. The full system of eight ODEs Eq. (18) has been solved, and the chiralities Eq. (19) calculated and plotted. We note that the two monomer chiralities ( $\mu$  and  $\chi$ ) remain in phase, with that of the activated monomer being larger ( $\chi$ ), as expected from the adiabatic approximation Eq. (50). The chiralities of the two dimers are phase-shifted by different amounts, and both have smaller amplitudes.

For the set of parameter values used in Fig. 4,  $a_c = 1.807$ , which gives  $w = 1.18$  and a time period of 5.3. The time period measured from the figure suggests a time period of 3.95; the discrepancy being due to the chosen value of  $a$  being reasonably far away from the bifurcation point, and possibly in accuracies due to the adiabatic approximation.

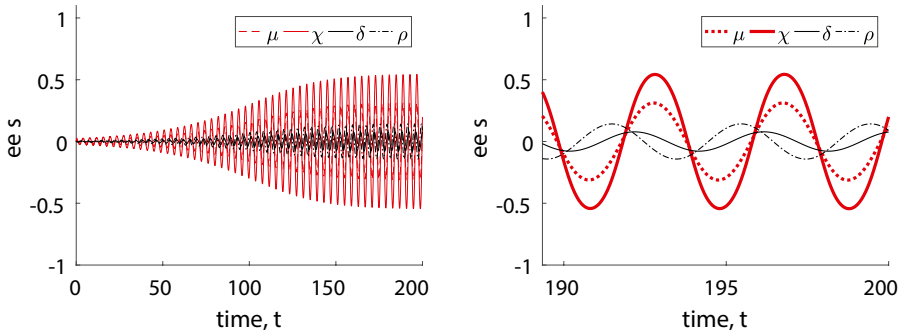


**Fig. 4** Illustration of oscillatory solutions of the dimer APED system. Parameter values:  $e = h = b = 1$ ,  $a = 10$ ,  $p = 5$ ,  $\alpha = 30$ ,  $\beta = 0.3$ ,  $\gamma = 0.3$ ,  $\mathcal{M} = 10$ . The initial conditions used were:  $L_1 = \frac{1}{2}\mathcal{M}(1 - \epsilon)$ ,  $R_1 = \frac{1}{2}\mathcal{M}(1 + \epsilon)$ ,  $\epsilon = 0.001$ ,  $R_2 = L_2 = P_2 = Q_2 = L_1^* = R_1^* = 0$ . (Figure, in color in online version.)

### Summary

In this section we have demonstrated the presence of asymmetric steady-state solutions, and oscillatory solutions, which are produced due to pitchfork and Hopf bifurcations. Whilst this behaviour has been observed in many previous works, we believe this is the first time that explicit expressions such as Eqs. (39), (40) and (53) have been generated. Understanding how the various rates ( $a, b, h, p, e$ ) and fidelities ( $\alpha, \beta, \gamma$ ) interact is critical in understanding experimental systems which may exhibit chiral symmetry-breaking behaviour.

In both adiabatic approximations the chirality of the activated species has emerged as the ‘fast’ variable, although this was not *a priori* assumed. The asymptotic assumptions made were that of large mass, and large  $\alpha$ . However, in both cases, this led to  $\chi$  adopting a pseudo-steady-state, and the instability was amplified since this satisfied  $\chi = k\mu$  with the constant of proportionality satisfying  $k > 1$ , indicating that the chiral monomers rapidly adapt to a larger  $ee$  than the unactivated monomers, which leads to the formation of more dimers. If this effect were to persist to systems which allowed longer polymers to form, this would drive the formation of longer homopolymers (growth) as well as the ‘nucleation’ of dimers.

### Conclusions

In this paper we have reviewed the literature on homochiralisation focusing on the viewpoint of mathematical models of physical processes. We started with a high level overview of the historical motivation from origins of life studies, and general ‘open’ models which exhibited both racemic and symmetry-breaking states. In "[Chiral Crystallisation Experiments](#)" we then focused on a few illustrative examples, namely the model of Sandars (2003) (see "[Sandars](#)"), and explanations of the crystal grinding experiments of Viedma (2005).

The latter part of the paper has concentrated on the APED model proposed by (Plasson et al. 2004). In "[The APED Model](#)" we reviewed the literature, and in "[Adiabatic Approximations in APED](#)" we presented new results on the bifurcation structure of the dimer

model for general parameter values. We used asymptotic analysis to separate the timescales for some processes, using adiabatic approximations to simplify the analysis. In both examples, the chirality of the activated monomers was the fast timescale, and allowed amplification of the  $ee$  which led to instability of the racemic state. For small  $\beta, \gamma$  and  $0 < \alpha < 1$  we found asymmetric steady-state could be stabilised via a pitchfork bifurcation; and for  $\alpha \gg 1$  we found that oscillatory solutions were created through a Hopf bifurcation.

In future work (Diniz et al. 2022) we generalise the results of "Adiabatic Approximations in APED" to a version of the APED reaction scheme in which arbitrarily long polymers can form, to complement and broaden the understanding of these systems that has been provided by Brandenburg et al. (2008), Plasson et al. (2004), Stich et al. (2013), and Bock and Peacock-Lopez (2020).

**Author Contributions** PD drafted the literature review "Introduction", "Origins", "Chiral Crystallisation Experiments", and "The APED Model". JW undertook the analysis presented in "Adiabatic Approximation in APED", and contributed to parts of "Introduction", "Origins", "Chiral Crystallisation Experiments", and "The APED Model". FC, JW and PD commented on drafts of "Introduction", "Origins", "Chiral Crystallisation Experiments", "The APED Model" and reviewed the manuscript.

**Funding** Not applicable.

**Data Availability** Not applicable.

## Declarations

**Ethics Approval** Not applicable.

**Consent for Publication** All the material presented here is owned by the authors and no permissions are required

**Conflicts of Interest** The authors confirm that they know of no conflicts of interest.

**Open Access** This article is licensed under a Creative Commons Attribution 4.0 International License, which permits use, sharing, adaptation, distribution and reproduction in any medium or format, as long as you give appropriate credit to the original author(s) and the source, provide a link to the Creative Commons licence, and indicate if changes were made. The images or other third party material in this article are included in the article's Creative Commons licence, unless indicated otherwise in a credit line to the material. If material is not included in the article's Creative Commons licence and your intended use is not permitted by statutory regulation or exceeds the permitted use, you will need to obtain permission directly from the copyright holder. To view a copy of this licence, visit <http://creativecommons.org/licenses/by/4.0/>.

## References

- Blackmond DG (2008) Response to Comment on A Re-Examination of Reversibility in Reaction Models for the Spontaneous Emergence of Homochirality. *J Phys Chem B* 112(31):9553–9555. <https://doi.org/10.1021/jp8040378>
- Becker R, Döring W (1935) Kinetische behandlung der keimbildung in übersättigten dämpfen. *Ann Phys* 24:719–752
- Blanco C, Hochberg D (2012) Homochiral oligopeptides by chiral amplification: interpretation of experimental data with a copolymerization model. *Phys Chem Chem Phys* 14(7):2301–2311. <https://doi.org/10.1039/C2CP22813K>
- Blanco C, Stich M, Hochberg D (2017) Mechanically induced homochirality in nucleated enantioselective polymerization. *J Phys Chem B* 121(5):942–955. <https://doi.org/10.1021/acs.jpcc.6b10705>
- Brandenburg A (2019) The limited roles of autocatalysis and enantiomeric cross-inhibition in achieving homochirality in dilute systems. *Orig Life Evol Biosph* 49:49–60. <https://doi.org/10.1007/s11084-019-09579-4>

- Brandenburg A, Andersen AC, Hofner S, Nilsson M (2005) Homochiral growth through enantiomeric cross-inhibition. *Orig Life Evol Biosph* 35:225–241. <https://doi.org/10.1007/s11084-005-0656-9>
- Brandenburg A, Lehto HJ, Lehto KM (2008) *Astrobiology*. Oct 2007:725–732. <https://doi.org/10.1089/ast.2006.0093>
- Bock W, Peacock-Lopez E (2020) Chiral oscillations and spontaneous mirror symmetry breaking in a simple polymerization model. *Symmetry* 12:1388. <https://doi.org/10.3390/sym12091388>
- Chen Y, Ma W (2020) The origin of biological homochirality along with the origin of life. *PLoS Comput Biol* 16(1). <https://doi.org/10.1371/journal.pcbi.1007592>
- Coveney PV, Swadling JB, Wattis JAD, Greenwell HC (2012) Theory, Modelling and Simulation in Origins of Life Studies. *Chem Soc Rev* 41:5430–5446
- Danger G, Plasson R, Pascal R (2010) An experimental investigation of the evolution of chirality in a potential dynamic peptide system: N-terminal epimerisation and degradation into diketopiperazine. *Astrobiology* 10:651–662
- Diniz PC, Wattis JAD, da Costa FP (2023) in preparation
- Eigen M (1971) Selforganization of matter and the evolution of biological macromolecules. *Die Naturwissenschaften*. 58(10):465–523. <https://doi.org/10.1007/BF00623322>
- Eigen M, Schuster P (1982) Stages of emerging life - five principles of early organization. *J Mole Evol* 19(1):47–61. <https://doi.org/10.1007/BF02100223>
- Frank FC (1953) On spontaneous asymmetric synthesis. *Biochimica et Biophysica Acta* 11:459–463. [https://doi.org/10.1016/0006-3002\(53\)90082-1](https://doi.org/10.1016/0006-3002(53)90082-1)
- Fuks G, Talom RM, Gauffre F (2011) Biohybrid block copolymers: towards functional micelles and vesicles. *Chem. Soc Rev* 40:2475–2493. <https://doi.org/10.1039/C0CS00085J>
- Girard C, Kagan HB (1998) Nonlinear Effects in Asymmetric Synthesis and Stereoselective Reactions: Ten Years of Investigation. *Angewandte Chemie International Edition* 37(21):2922–2959. <https://pubmed.ncbi.nlm.nih.gov/29711141/>
- Gleiser M, Walker S-I (2009) Toward homochiral protocells in noncatalytic peptide systems. *Orig Life Evol Biosph* 39:479–493
- Gleiser M, Walker SI (2008) An extended model for the evolution of prebiotic homochirality: a bottom-up approach to the origins of life. *Orig Life Evolution Biosph* 38(4):293–315. <https://doi.org/10.1007/s11084-012-9274-5>
- Gleiser M, Nelson BJ, Walker SI (2012) Chiral polymerisation inopen systems from chiral-selective reaction rates. *Orig Life Evol Biosph* 42(4):333–346
- Haldane JBS (1929) The origin of life. *Rationalist Annual* 3:148–153
- Hitz T, Blocher M, Walde P, Luisi PL (2001) Stereoselectivity aspects in the condensation of racemic NCA-amino acids in the presence and absence of liposomes. *Macromolecules* 34(8):2443–2449. <https://doi.org/10.1021/ma001946w>
- Hochberg D, Bourdon Garcia RD, Agreda Bastidas JA, Ribo JM (2017) Stoichiometric network analysis of spontaneous mirror symmetry breaking in chemical reactions. *Phys Chem Chem Phys* 19:17618–17636. <https://doi.org/10.1039/C7CP02159C>
- Kipping FS, Pope WJ (1898a) LXIII - Enantiomorphism *J Chem Soc Trans* 73(0):606–617. <https://doi.org/10.1039/ct8987300606>
- Kipping FS, Pope WJ (1898b) Stereochemistry and vitalism. *Nature* 59(1516):53. <https://doi.org/10.1038/059053b0>
- Kondepudi DK, Kaufman RJ, Singh N (1990) Chiral symmetry-breaking in Sodium Chlorate Crystallization. *Science* 250(4983):975–976. <https://doi.org/10.1126/science.250.4983.975>
- Konstantinov KK, Konstantinova AF (2020) Chiral symmetry breaking in large peptide systems. *Orig Life Evol Biosph* 50:99–120. <https://doi.org/10.1007/s11084-020-09600-1>
- Laurent G, Gaspard P, Lacoste D (2022) Arobust transition to homochirality in complex chemical reaction networks. *Proc Roy Soc Lond A*:478(2257)
- Lazcano A, Bada JL (2003) The 1953 Stanley L. Miller experiment: fifty years of prebiotic organic chemistry *Orig Live Evol Biosph* 33(3):235–242. <https://doi.org/10.1023/a:1024807125069>
- McBride JM, Carter RL (1991) Spontaneous Resolution by Stirred Crystallization. *Angewandte Chemie International Edition in English* 30(3):293–295. <https://doi.org/10.1002/anie.199102931>
- McBride JM, Tully JC (2008) Did life grind to a start? *Nature* 452(7184):161–162. <https://doi.org/10.1038/452161a>
- Miller SL (1953) A production of amino acids under possible primitive earth conditions. *Science* 117(3046):528–529. <https://doi.org/10.1126/science.117.3046.528>
- Montoya A, Cruz E, Agreda J (2019) Computing the Parameter Values for the Emergence of Homochirality in Complex Networks. *Life* 9:74. <https://doi.org/10.3390/life9030074>
- Murray JD (1989) *Mathematical Biology, Biomathematics*, vol 19. Springer, Berlin

- Noorduyn WL, Izumi T, Millemaggi A, Leeman M, Meekes H, Van Enckevort WJP, Kellogg RM, Kaptein B, Vlieg E, Blackmond DG (2008) Emergence of a Single Solid Chiral State from a Nearly Racemic Amino Acid Derivative. *J Am Chem Soc* 130(4):1158–1159. <https://doi.org/10.1021/ja7106349>
- Oparin AI (1938) *The Origin of Life*. Dover, New York
- Plasson R (2008) Comment on Re-Examination of Reversibility in Reaction Models for the Spontaneous Emergence of Homochirality. *J Phys Chem B* 112(31):9550–9552. <https://doi.org/10.1021/jp803588z>
- Plasson R, Bersini H, Commeyras A (2004) Recycling Frank: Spontaneous emergence of homochirality in noncatalytic systems. *Proc Nat Acad Sci* 101:16733–16738. <https://doi.org/10.1073/pnas.0405293101>
- Plasson R, Kondepudi D, Bersini H, Commeyras A, Asakura K (2007) Emergence of homochirality in far-from-equilibrium systems: Mechanisms and role in prebiotic chemistry. *Chirality* 19(8):589–600. <https://doi.org/10.1002/chir.20440>
- Ribo JM, Crusats J, El-Hachemi Moyano A, Hichberg D (2017) Spontaneous mirror symmetry breaking in heterocatalytically coupled enantioselective replicators. *Chem Sci* 8:763–769. <https://doi.org/10.1039/c6sc02446g>
- Ribo JM, Hochberg D, Crusats J, El-Hachemi Z, Moyano A (2017) Spontaneous mirror symmetry breaking and origin of biological homochirality. *J Roy Soc Interface* 14(137):20170699. <https://doi.org/10.1098/rsif.2017.0699>
- Saito Y, Hyuga H (2004) Complete homochirality induced by nonlinear autocatalysis and recycling. *J Phys Soc Japan* 73:33–35. <https://doi.org/10.1143/jpsj.73.33>
- Saito Y, Hyuga H (2005) Chirality Selection in Crystallization. *J Phys Soc Japan* 74:535–537. <https://doi.org/10.1143/jpsj.74.535>
- Saito Y, Hyuga H (2013) Homochirality: Symmetry breaking in systems driven far from equilibrium. *Rev Mod Phys* 85:603
- Sandars PGH (2003) A toy model for the generation of homochirality during polymerization. *Orig Life Evol Biosph* 33(6):575–587. <https://doi.org/10.1023/a:1025705401769>
- Soai K, Shibata T, Morioka H, Choji K (1995) Asymmetric autocatalysis and amplification of enantiomeric excess of a chiral molecule. *Nature* 378(6559):767–768. <https://doi.org/10.1038/378767a0>
- Stich M, Blanco C, Hochberg D (2013) Chiral and chemical oscillations in a simple dimerization model. *Phys Chem Chem Phys* 15:255–261. [arXiv.org/abs/1210.1872](https://arxiv.org/abs/1210.1872)
- Tsogoeva SB, Wei S, Freund M, Mauksch M (2009) Generation of highly enantioenriched crystalline products in reversible asymmetric reactions with racemic or achiral catalysts. *Angewandte Chemie International Edition* 48:590–594. <https://doi.org/10.1002/anie.200803877>
- Uwaha M (2004) A Model for Complete Chiral Crystallization. *J Phys Soc Japan* 73(10):2601–2603. <https://doi.org/10.1143/jpsj.73.2601>
- Urey HC (1952) On the early chemical history of the earth and the origin of life. *Proceedings of the National Academy of Sciences* 38(4):351–363. <https://doi.org/10.1073/pnas.38.4.351>
- Viedma C (2005) Chiral symmetry-breaking During Crystallization: Complete Chiral Purity Induced by Nonlinear Autocatalysis and Recycling. *Phys Rev Lett* 94(6). <https://doi.org/10.1103/physrevlett.94.065504>
- Viedma C, Cintas P (2011) Homochirality beyond grinding: deracemizing chiral crystals by temperature gradient under boiling. *Chem Commun* 47:12786–12788. <https://doi.org/10.1039/c1cc14857e>
- Walker SI (2017) Origins of life: a problem for physics, a key issues review. *Rep Prog Phys* 80. <https://doi.org/10.1088/1361-6633/aa7804>
- Wattis JAD (2010) Mathematical models of the homochiralisation of crystals by grinding. *Origins of Life and Evolution of Biospheres* 41:133–173
- Wattis JAD, Coveney PV (2007) Sequence selection during copolymerisation. *J Phys Chem* 111:9546–9562
- Wattis JAD, Coveney PV (2005a) Symmetry-breaking in chiral polymerisation. *Orig Life Evol Biosph* 35:243–273. [arXiv.org/abs/physics/0402091](https://arxiv.org/abs/physics/0402091)
- Wattis JAD, Coveney PV (2005b) Chiral polymerisation and the RNA world. *Int J Astrobiology* 4:63–73